†Supplementary material

Two novel six-coordinated cadmium (II) and zinc (II) complexes from carbazate *β*-diketonate: crystal structures, enhanced two-photon absorption and biological imaging application†

Cuiyun Nie,‡ [a] Qiong Zhang,‡ [a] Hongjuan Ding,[b] Bei Huang,[c] Xinyan Wang,[c] Xianghua Zhao,[a] Shengli Li,[a] Hongping Zhou,[a] Jieying Wu,*,[a] Yupeng Tian[a,d,]*

[a] *Department of Chemistry, Key Laboratory of Functional Inorganic Materials Chemistry of Anhui Province, Anhui University, Hefei 230039, P. R. China* E-mail: jywu1957@163.com; yptian@ahu.edu.cn

[b] *Department of Physics, Shandong Normal University, Jinan 250014, P. R. China*

[c] *Department of Biology, Anhui University, Hefei 230039, P. R. China*

[d] *State Key Laboratory of Coordination Chemistry, Nanjing University, Nanjing, 210093, P. R. China*

†*Dedicated to Professor Xiao-Zeng You for His 80th Birthday*;

‡ *These authors contributed equally to this work.*

Legands

Fig. S1. The variable temperature ^{1}H NMR of **Zn(II)L_2(H_2O)$_2$** has been measured in order to further prove the stability of the complex in DMSO.

Fig. S2.MALDI-TOF Mass spectrometry was used to further verify the stability of complex **Zn(II)L_2(H_2O)$_2$** in water solution, which first dissolved in a small amount of DMF, and then diluted with water.

Fig. S3. The extended electron delocalization was confirmed by XPS from an experimental viewpoint. XPS result shows the atomic concentration sequence of O atom is Cd(II)L_2(H_2O)$_2$ (16.89) >Zn(II)L_2(H_2O)$_2$ (13.78) >HL (12.12) which was in accordance with the electron delocalization tendency.

Fig. S4. The abbreviated diagram of MO theory.

Fig. S5. Enlarged diagrams of the molecular orbital of **HL**

Fig. S6. Computation results of the **Zn(II)L_2(H_2O)$_2$**

Table S1 Crystal data and structure refinement for **Cd(II)L_2(H_2O)$_2$** and **Zn(II)L_2(H_2O)$_2$**.

Table S2 Selected bond lengths (Å) and angles (°) for **Cd(II)L_2(H_2O)$_2$** and **Zn(II)L_2(H_2O)$_2$**.

Table. S3. TD-DFT computational studies were performed to elucidate the electronic structures of the ground state of HL, Cd(II)L_2(H_2O)$_2$ and Zn(II)L_2(H_2O)$_2$.

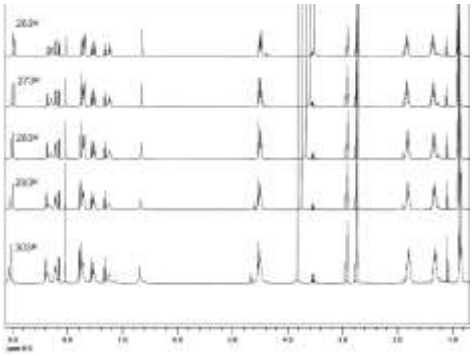

Fig. S1. Variable temperature ^{1}H NMR spectra of **Zn(II)L$_2$(H$_2$O)$_2$**.

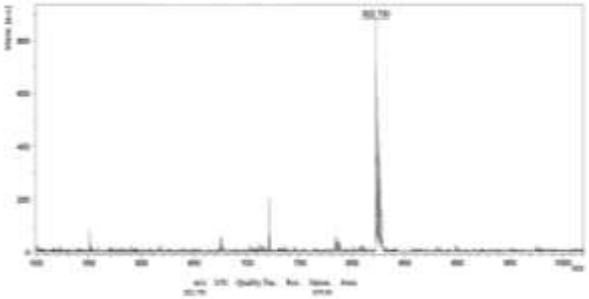

Fig. S2. MALDI-TOF mass spectra of **Zn(II)L$_2$(H$_2$O)$_2$**.

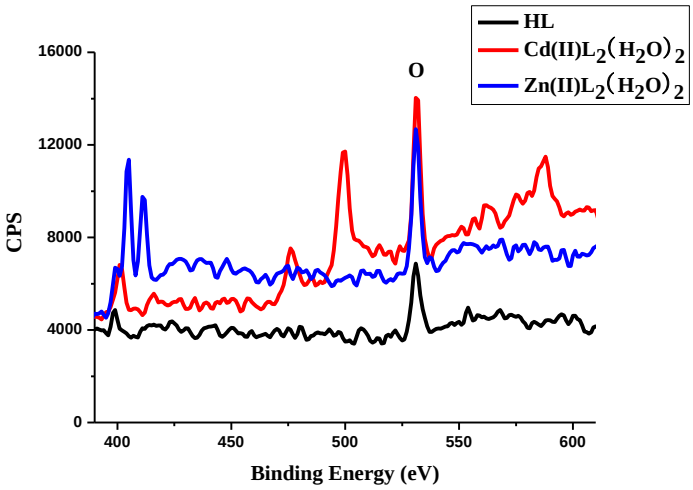

Fig. S3. XPS spectra of all the compounds

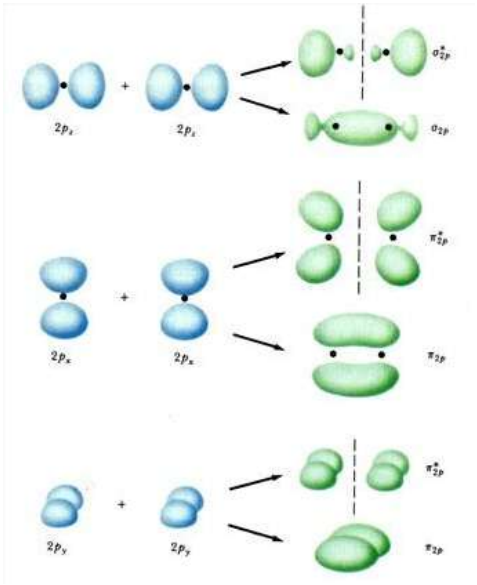

Fig. S4. The abbreviated diagram of MO theory.

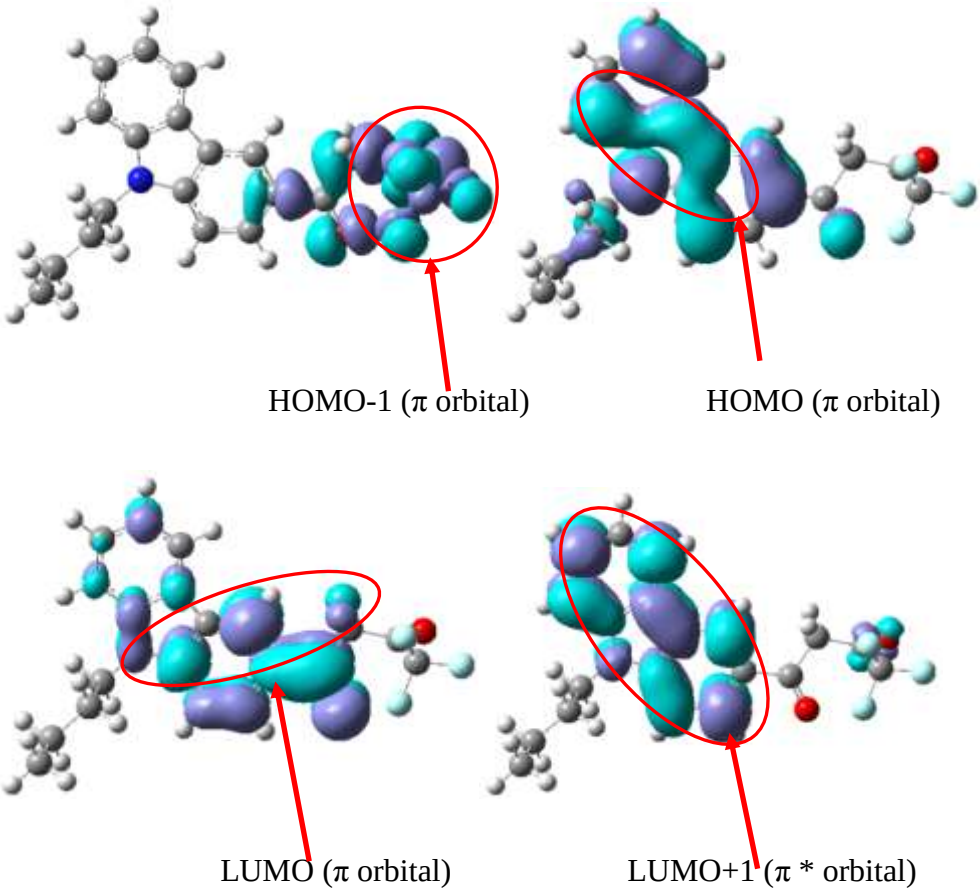

Fig. S5. Enlarged diagrams of the molecular orbital of HL

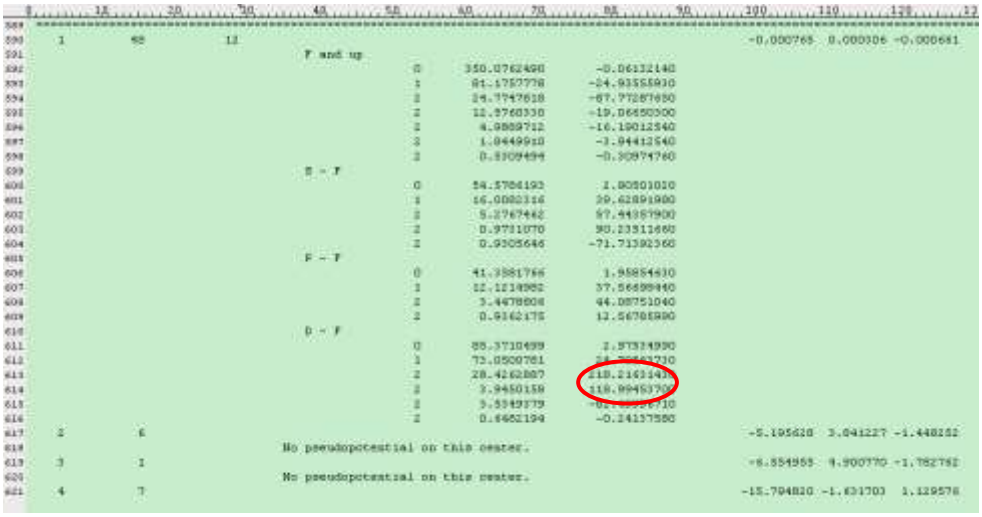

Fig. S6. Computation results of the $Zn(II)L_2(H_2O)_2$

Table S1 Crystal data and structure refinement for **$Cd(II)L_2(H_2O)_2$** and **$Zn(II)L_2(H_2O)_2$**.

Compound	**$Cd(II)L_2(H_2O)_2$**	**$Zn(II)L_2(H_2O)_2$**
Empirical formula	C40 H38 F6 N2 O4 Cd	C40 H38 F6 N2 O4 Zn
Formula weight	869.12	822.09
Crystal system	Monoclinic	Monoclinic
Space group	C2/c	C2/c
Temperature (K)	293(2)	273(2)
λ of Mo-K_α [Å]	0.71	0.71
Absorption coefficient[mm^{-1}]	0.06	0.06
Unit cell dimensions	a =39.67(9) Å b=5.34(10) Å c =20.25(5) β=104.29(2) °	a =39.08(13) Å b=5.27(2)Å c =20.21(6)Å β=103.91(2)°
V [$Å^3$]	4158.47(16)	4039.00(2)
Reflections collected	15154	13298
Reflections unique	4752	3527
R_{int}	0.0321	0.0666
R_1	0.0646	0.0932
wR_2	0.2065	0.2804
Goodness of fit on F^2	1.080	1.102

Table S2 Selected bond lengths (Å) and angles (°) for **$Cd(II)L_2(H_2O)_2$** and **$Zn(II)L_2(H_2O)_2$**.

$Cd(II)L_2(H_2O)_2$			
Cd(1)-O(3)	2.361(3)	O(5)-Cd(1)-O(5)#1	180.00(11)

Cd(1)-O(5)	2.227(3)	O(5)-Cd(1)-O(6)	83.37(11)
Cd(1)-O(6)	2.230(3)	O(5)-Cd(1)-O(6)#1	96.63(11)
C(22)-C(23)	1.367	O(5)-Cd(1)-O(3)#1	87.54(12)
C(23)-C(24)	1.420	O(5)-Cd(1)-O(3)	92.46(12)
C(22)-O(6)	1.279		
C(24)-O(5)	1.257		
Zn(II)$L_2(H_2O)_2$			
Zn(1)-O(1)	2.053(5)	O(2)-Zn(1)-O(2)#1	180.00(17)
Zn(1)-O(2)	2.033(5)	O(2)-Zn(1)-O(1)#1	90.19(19)
Zn(1)-O(3)	2.239(5)	O(2)-Zn(1)-O(1)	89.81(19)
C(17)-C(18)	1.424	O(2)-Zn(1)-O(3)#1	90.6(2)
C(18)-C(19)	1.323	O(2)-Zn(1)-O(3)	89.4(2)
C(19)-O(2)	1.282		
C(17)-O(1)	1.256		

Table S3 Excitation energies (*E*), corresponding wavelengths (λ), oscillator strengths (*f*) and major contributors for **HL**, **Cd(II)$L_2(H_2O)_2$** and **Zn(II)$L_2(H_2O)_2$** [a]**. (** [a] Only the transitions with a calculated oscillator strength higher than 0.0010 are reported.**)**

	E (eV)	λ (nm)	f	Composition	Character
HL	3.48	356.27	0.0009	93(H-1)→97(L+2)(0.6101 2)	π→ π*
	4.49	275.92	0.2032	94(H)→95（L)（0.56918)	n→ π*
Cd(II)$L_2(H_2O)_2$	3.50	353.91	0.0011	202(H-1)→204(L)(0.5948 1)	π→ π* MLCT
	4.47	277.16	0.2742	202(H-1)→206(L+2) (0.29774)	n→ π*
Zn(II)$L_2(H_2O)_2$	3.95	351.00	0.0021	203(H)→204(L)（0.57055)	π→ π* MLCT
	4.37	283.63	0.0072	203(H)→207(L+3) (0.60174)	n→ π*

According to the MO theory and the abbreviated diagram, we can clearly see that the π orbital was a distorted ellipsoid and the π * orbital was a distorted ball. Hense, from the Figure 4 in the main text, **t**he HOMOs (H) and H-1 of HL are of π orbitals localized on the carbazole and COCHC(OH)CF_3 groups. The unoccupied molecular orbitals LUMO (L) and L+1 are of the π * orbital localized on carbazole and COCHC(OH)C_6H_5 units which was in line with the MO theory. For complexes Zn(II)$L_2(H_2O)_2$ as an example, the d orbitals can hardly be intuitively from the diagram, however, the computation result can be provided to prove the metal ion hybidized d,s,p-orbitals. From Fig. S6, we can clearly see that the d-orbitals of Zn (II) has highest coefficient (218.21 and 118.99).